

EVIDENCE FOR PRODUCTION OF AN  $N^*(1400)$  AND  $\bar{N}^*(1400)$   
 IN THE REACTION  $\bar{p}p(n) \rightarrow \bar{p}p\pi^+\pi^-(n)$  AT 2.8 GeV/c\*

T. C. Bacon,<sup>†</sup> F. Bomse, T. B. Borak, T. B. Cochran,<sup>‡</sup>  
 W. J. Fickinger,<sup>§</sup> E. R. Goza,<sup>||</sup> H. W. K. Hopkins,<sup>\*\*</sup> and E. O. Salant  
 Department of Physics, Vanderbilt University, Nashville, Tennessee

(Received 11 October 1968)

In the reaction  $\bar{p}p(n) \rightarrow \bar{p}p\pi^+\pi^-(n)$  at 2.8 GeV/c, enhancements in the mass spectra of  $\bar{p}\pi^-\pi^+$  and  $p\pi^-\pi^+$  have been observed near 1400 MeV. Analysis indicates that these enhancements cannot be adequately explained as kinematic reflections of  $N^*(1238)$  and/or  $\bar{N}^*(1238)$  production.

Several counter groups<sup>1</sup> have observed enhancements between 1400 and 1450 MeV in the missing-mass spectrum from the reaction  $p\bar{p} \rightarrow p +$  (missing mass). Several bubble-chamber groups<sup>2</sup> have also reported the observation of similar enhancements in the mass spectra of  $T_z = \frac{1}{2} N\pi$  and  $N\pi\pi$  systems produced in  $p\bar{p}$ ,  $Kp$ , and  $\pi p$  collisions. These peaks are generally associated with small four-momentum transfer to the missing-mass or nucleon-pion system in question and have been interpreted either as evidence for the  $P_{11}$  resonance predicted by Roper<sup>3</sup> or as kinematic reflections. In this Letter we report the observation of enhancements near 1400 MeV in the  $\bar{p}\pi^-\pi^+$  and  $p\pi^-\pi^+$  mass distributions from the reaction  $\bar{p}d \rightarrow \bar{p}p\pi^+\pi^-$  at 2.8-GeV/c incident antiproton momentum.

Our analysis is based on events of the type  $\bar{p}p(n) \rightarrow \bar{p}p\pi^+\pi^-(n)$ . There are, in addition, indications of similar enhancements in the  $\bar{p}\pi^-\pi^+$  and  $n\pi^-\pi^+$  mass spectra from the companion reaction  $\bar{p}n(p) \rightarrow \bar{p}n\pi^+\pi^-(p)$ . However, the possibility of producing the  $N^{*-}(1238)$  or  $\bar{N}^{*-}(1238)$  isobars in either the  $n\pi^-$  or  $\bar{p}\pi^-$  systems in that reaction complicates the analysis somewhat and we shall defer consideration of it to a future publication.

The events in our sample were obtained from approximately 14 500 four-pronged events observed in the Brookhaven National Laboratory deuterium-filled 20-in. bubble chamber exposed to a 2.8-GeV/c antiproton beam at the alternating-gradient synchrotron. We discuss only events in which the neutron momentum is less than 250 MeV/c, a range in which the impulse approximation appears valid.<sup>4</sup> The 602 events for which this restriction is satisfied correspond to a total section for the reaction  $\bar{p}p(n) \rightarrow \bar{p}p\pi^+\pi^-(n)$  of  $1.7 \pm 0.2$  mb.

This reaction is apparently dominated by the production of the  $\bar{N}^{*-}(1238)$  and  $N^{*+}(1238)$  resonances. The mass distributions of the  $\bar{p}\pi^-$  and

$p\pi^+$  systems are shown in Figs. 1(a) and 1(b). The triangle scatter plot of  $M_{\bar{p}\pi^-}$  vs  $M_{p\pi^+}$  (not shown) indicates strong simultaneous production of the  $\bar{N}^{*-}$  and  $N^{*+}$ . In addition, there are enhancements in the isobar bands outside the cross-over region, indicating single isobar production as well. We estimate that this resonance formation involves about 72% of the events. Furthermore, examination of the scatter plot of  $M_{p\pi^+}$  vs  $M_{p\pi^-}$  shows no evidence for production of either  $\bar{N}^{*0}(1238)$  or  $N^{*0}(1238)$ . The production angular distribution for the  $\bar{p}\pi^-$  and  $p\pi^+$  systems in the overall center-of-mass frame shown in Fig. 1(c) reveals the peripheral nature of the interaction. In view of these results we assume a model for the reaction which consists of an incoherent sum of the squared matrix element corresponding to the single-pion-exchange diagram shown in Fig. 1(d) and Lorentz-invariant phase space, taken in the proportions 72 to 28%, respectively. We note, however, that the conclusions we shall subsequently draw from this analysis are insensitive (to within  $\pm 20\%$ ) to this choice of weights.

The single-pion-exchange part of the cross section is proportional to  $|V_I|^2 F(\Delta^2) |V_{II}|^2$ . Here  $V_I$  and  $V_{II}$  are vertex functions corresponding to the shaded circles of Fig. 1(d). In our calculation they are taken to be

$$|V|^2 = (8\pi\omega)^2 d\sigma(\omega, \cos\theta)/d\Omega. \quad (1)$$

In (1),  $V$  is either  $V_I$  or  $V_{II}$  and  $\omega$  is either the  $\bar{p}\pi^-$  or  $p\pi^+$  effective mass. The term  $d\sigma(\omega, \cos\theta)/d\Omega$  is the on-mass-shell, elastic,  $T = \frac{3}{2}\pi - \theta$  differential cross section at effective mass  $\omega$ , expressed in terms of the scattering angle  $\theta$  between the incoming  $\bar{p}$  ( $p$ ) and outgoing  $\bar{p}$  ( $p$ ) in the  $\bar{p}\pi^-$  ( $p\pi^+$ ) rest frame. The absence of any dependence of  $d\sigma/d\Omega$  on azimuthal angle is consistent with the observation that the experimental Treiman-Yang distributions (not shown) are flat. We are assuming that the on-mass-shell differential cross sections provide an adequate representa-

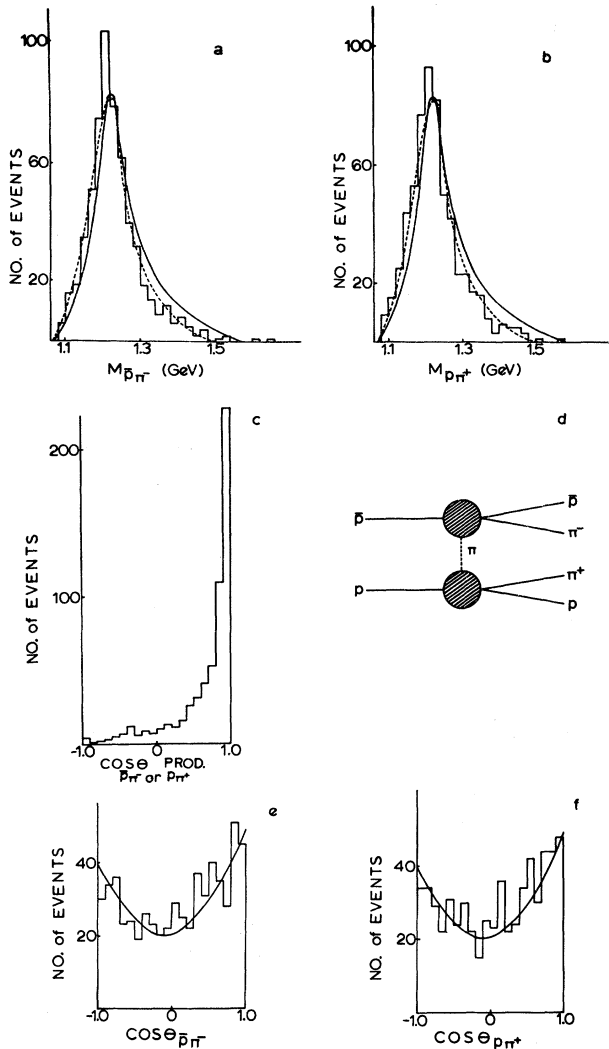


FIG. 1. (a) and (b) The  $\bar{p}\pi^-$  and  $p\pi^+$  mass distribution. The solid curves are the prediction of a model involving no  $\bar{N}^*(1400)$  or  $N^*(1400)$  production (model 1). The dashed curves are the predictions of a model involving production of both the  $\bar{N}^*(1400)$  and  $N^*(1400)$  (model 2). (c) The production angular distribution of the  $\bar{p}\pi^-$  ( $p\pi^+$ ) system in the overall center-of-mass system. (d) The single-pion-exchange diagram used in both models. (e) and (f) Scattering angular distributions of the outgoing  $\bar{p}$  ( $p$ ) with respect to the incoming  $\bar{p}$  ( $p$ ) in the  $\bar{p}\pi^-$  ( $p\pi^+$ ) rest frame. The solid curves are the predictions of model 1.

tion of the off-mass-shell differential cross sections at corresponding values of  $\omega$ . The function  $F(\Delta^2)$  contains the pion propagator and any form factors connected with vertex and propagator corrections. Here  $\Delta^2$  is the squared four-momentum transfer from the incoming  $\bar{p}$  ( $p$ ) to the outgoing  $\bar{p}\pi^-$  ( $p\pi^+$ ) system. To calculate the contribution of the single-pion-exchange diagram we have ex-

pressed the differential cross sections in terms of power series expansions in  $\cos\theta$  taken directly from elastic pion-proton scattering data.<sup>5</sup> For  $F(\Delta^2)$  we have chosen a function which reproduces our experimental  $\Delta^2$  distributions. We have used these parameters as input to a Monte Carlo program which calculates all mass and angular distributions of interest. To these we add, in suitable proportion, the corresponding phase-space distributions arising from the constant part of the complete matrix element of our model.

We find that the experimental  $\bar{p}\pi^-$  and  $p\pi^+$  mass distributions shown in Figs. 1(a) and 1(b), as well as the distributions in scattering angle between the incoming  $\bar{p}$  ( $p$ ) and outgoing  $\bar{p}$  ( $p$ ) [Figs. 1(e) and 1(f)], are in good agreement with the predictions of this model, which are indicated by the solid curves.

We now turn to the three-body mass distributions shown in Figs. 2(a) and 2(b), where the results of the Monte Carlo calculation are again indicated by the solid curves. There are statistically significant discrepancies between the histograms and the curves in the low-mass regions. We also note at this point the qualitative similarity of the smooth curves to the predictions of Lorentz-invariant phase space, confirming our earlier remark that the results are insensitive to the particular weights we have assigned.

We have also calculated a model in which the input parameters to the Monte Carlo program corresponded to the absorptive single-pion-exchange model of Jackson.<sup>6</sup> This calculation involved production amplitudes for the quasi-two-body reactions  $\bar{p}p \rightarrow \bar{N}^{*--}(1238)N^{*++}(1238)$ ,  $\bar{p}p \rightarrow \bar{N}^{*--}(1238)p\pi^+$ , and  $\bar{p}p \rightarrow N^{*++}(1238)\bar{p}\pi^-$ . There were no differences between the results of this calculation and those of the calculation described above. In fact, for any single-particle-exchange diagram of the type shown in Fig. 1(d), the angular distributions  $d\sigma(\omega, \cos\theta)/d\Omega$  would have to be proportional to  $1 + 10 \cos^2\theta$  over the entire range of  $\omega$  in order to reproduce the 1400-MeV enhancements in the three-body mass spectra.

Of various possibilities for understanding the results of Figs. 2(a) and 2(b) we proceed to investigate a model which, in addition to the diagram of Fig. 1(d), includes amplitudes for production of both an  $\bar{N}\pi\pi$  and  $N\pi\pi$  state near 1400 MeV. We calculate these squared amplitudes with our Monte Carlo program on the assumption that the 1400-MeV resonance decays isotropically into an  $N^*(1238)$  isobar and a pion with sub-

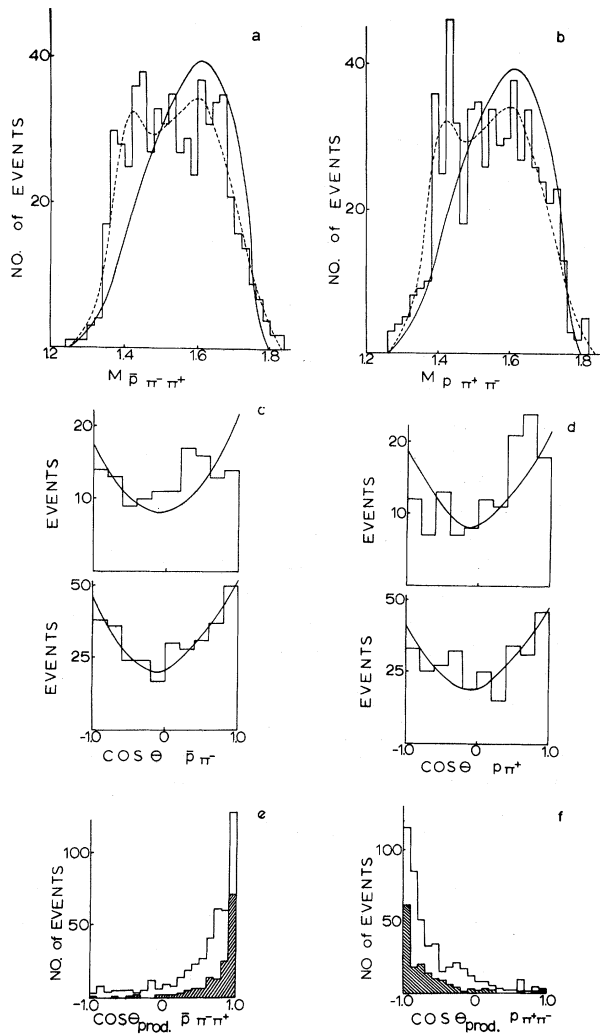


FIG. 2. (a) and (b) The  $\bar{p}\pi^-\pi^+$  and  $p\pi^-\pi^+$  mass distributions. The solid curves are the predictions of model 1. The dashed curves are the predictions of model 2. (c) and (d) The  $\bar{N}^*(1238)$  and  $N^{*++}(1238)$  decay angular distributions for events inside (upper histograms) and outside (lower histograms) the respective  $\bar{N}^*(1400)$  or  $N^*(1400)$  mass regions. The solid curves are the predictions of model 1. (e) and (f) Production angular distributions for the  $\bar{p}\pi^-\pi^+$  and  $p\pi^-\pi^+$  systems. The upper histograms contain events with  $\bar{p}\pi^-\pi^+$  or  $p\pi^-\pi^+$  mass outside the  $\bar{N}^*(1400)$  or  $N^*(1400)$  mass regions. The lower shaded histograms contain events with  $\bar{p}\pi^-\pi^+$  or  $p\pi^-\pi^+$  mass within the  $\bar{N}^*(1400)$  or  $N^*(1400)$  mass region.

sequent isotropic decay of the  $N^*(1238)$  (as we shall remark further on, however, we cannot rule out other possible modes of decay of the 1400-MeV enhancements). The distributions of the squared four-momentum transfer to the 1400-MeV systems were chosen in accordance with the corresponding experimental distributions [Figs.

2(e) and 2(f). Several different masses and widths for these resonances were used in the calculations. The model which best reproduces all of our data is one in which the reactions  $\bar{p}p \rightarrow \bar{N}^*(1400)p \rightarrow \bar{p}\pi^-\pi^+p$  and  $\bar{p}p \rightarrow N^*(1400)\bar{p} \rightarrow p\pi^-\pi^+\bar{p}$  each contribute 20% to the total cross section, and the single-pion-exchange diagram of Fig. 1(d) contributes 60%. The mass and width of the  $N^*(1400)$  systems are  $1400 \pm 10$  and  $80 \pm 20$  MeV, respectively. This mass value is somewhat lower than the centers of the experimental peaks, which occur closer to 1420 MeV as reference to Figs. 2(a) and 2(b) will confirm. The difference is explained by the fact that beneath the  $\bar{p}\pi^-\pi^+$  enhancement in Fig. 2(a) both the single-pion-exchange amplitude and the production amplitude for the  $N^*(1400)$  in the  $p\pi^-\pi^+$  system correspond to a  $\bar{p}\pi^-\pi^+$  mass distribution which slopes sharply upward to the right. This tends to shift the experimentally observed peak to a higher mass. A similar conclusion may be drawn for the  $p\pi^-\pi^+$  peak of Fig. 2(b). The predictions of the new model are shown as the dotted curves in Figs. 1(a), 1(b), 2(a), and 2(b). It is clear that all of the two- and three-body mass spectra are substantially better fitted by this model than by the original one. Moreover, we have compared the experimental scatter plot of  $M_{\bar{p}\pi^-}$  vs  $M_{p\pi^+}$  with a similar scatter plot of the Monte Carlo events generated according to the new model and obtain excellent agreement. There is also good agreement between this model and the two-body production and decay angular distributions.

The isotropic decays of the  $N\pi\pi(1400)$  state [ $N^*(1400)$ ] and the  $N^*(1238)$  prescribed by this model are consistent with a spin-and-parity assignment of  $\frac{1}{2}^+$  for the  $N\pi\pi$  enhancement. Positive identification of this enhancement with the  $P_{11}$  resonance of Roper is precluded because of the disagreement in mass and width. However, similar enhancements observed in other experiments<sup>1,2</sup> show a spectrum of masses and widths ranging from 1400 to 1450 MeV and from 50 to 250 MeV, respectively.

We now turn to the angular distributions of the 1400-MeV enhancements. If we assume a spin-and-parity assignment of  $\frac{1}{2}^+$  and the decay mode  $N^*(1400) \rightarrow N^*(1238)\pi$  [where the  $N^*(1238)$  has  $|T_z| = \frac{3}{2}$ ], then the  $N^*(1238)$  decay angular distributions given by  $d\sigma(\omega, \cos\theta)/d\Omega$  should tend to be flat when the corresponding  $N\pi\pi$  system is in the 1400-MeV region. This follows because the decay  $N^*(1400) \rightarrow N^*(1238)\pi$  must be isotropic in the  $N^*(1400)$  rest frame, and hence the subsequent

decay of the  $N^*(1238)$  must also be isotropic in its own rest frame when referred to the beam direction as quantization axis. In Figs. 2(c) and 2(d) we show the scattering angular distributions of the  $\bar{N}^{*--}(1238)$  and  $N^{*++}(1238)$  for events inside (upper histograms) and outside (lower histograms) the corresponding  $N^*(1400)$  bands, which are defined by  $1380 \text{ MeV} \leq M_{\bar{p}\pi-\pi^+}$  or  $M_{p\pi-\pi^+} \leq 1480 \text{ MeV}$ . For this purpose, the  $N^*(1238)$  bands were defined by  $1160 \text{ MeV} \leq M_{p\pi} \leq 1300 \text{ MeV}$ . The smooth curves represent the empirical elastic-scattering angular distributions of our original model integrated over the appropriate mass regions. This test is inconclusive although there is some suggestion that the  $\bar{N}^{*--}(1238)$  scattering distribution is closer to isotropy inside the  $\bar{N}^*(1400)$  band than outside, since the upper histogram of Fig. 2(c) is better fitted by a flat distribution. We have also investigated the possibility that the 1400-MeV enhancements may decay by the mode  $N^*(1400) \rightarrow N(\pi\pi)$ . Again the results are inconclusive, so that we cannot rule out either of the two assumptions.

As pointed out earlier, however, other experiments have shown that the 1400-MeV enhancement is associated with extremely peripheral interactions.<sup>1,2</sup> In Figs. 2(e) and 2(f) are shown the production angular distributions of the  $\bar{p}\pi-\pi^+$  and  $p\pi-\pi^+$  systems in the overall center-of-mass frame. The upper histograms contain only those events with the three-body mass outside the 1400-MeV region, while the lower shaded events have three-body mass within that region. We note that the latter are considerably more peripheral than the former, as might be expected if the shaded samples represent a three-body resonant state. Indeed, if in Fig. 2(e) one calculates the ratio of events in the first bin to all events for the lower and upper samples separately, one obtains 0.46 and 0.28, respectively. The corresponding ratios associated with Fig. 2(f) are 0.39 for the lower sample and 0.25 for the upper one.

We conclude from the above analyses that our data are consistent with the peripheral production of a resonant state in both the  $\bar{p}\pi-\pi^+$  and  $p\pi-\pi^+$  systems, with a mass of  $1400 \pm 10 \text{ MeV}$  and a width of  $80 \pm 20 \text{ MeV}$ .

We would like to thank the operating crews of the alternating-gradient synchrotron and the 20-in. bubble chamber and our scanning and measuring staff for their cooperation. We are indebted to Dr. E. J. Moses for his comments.

---

\*Work supported in part by a grant from the National Science Foundation, which is gratefully acknowledged.

†Present address: Rutherford High Energy Laboratory, Chilton, Didcot, Berkshire, England.

‡Present address: Physics Department, Navy Postgraduate School, Monterey, Calif.

§Present address: Physics Department, Case Western Reserve University, Cleveland, O.

||Present address: Physics Department, Louisiana State University, Baton Rouge, La.

\*\*Present address: CERN, Geneva, Switzerland.

<sup>1</sup>G. Cocconi *et al.*, *Phys. Letters* **8**, 134 (1964); C. M. Ankenbrandt *et al.*, *Nuovo Cimento* **35**, 1052 (1965); G. Belletini *et al.*, *Phys. Letters* **18**, 167 (1965); E. W. Anderson *et al.*, *Phys. Rev. Letters* **16**, 855 (1966); I. M. Blair *et al.*, *ibid.* **17**, 789 (1966); K. J. Foley *et al.*, *ibid.* **19**, 397 (1967).

<sup>2</sup>S. L. Adelman, *Phys. Rev. Letters* **13**, 555 (1964); Eugene Gellert *et al.*, *ibid.* **17**, 884 (1966); S. P. Almeida *et al.*, *Nuovo Cimento* **50A**, 1000 (1967); Robert B. Bell *et al.*, *Phys. Rev. Letters* **20**, 164 (1968); Edmund L. Berger, E. Gellert, G. A. Smith, E. Colton, and P. E. Schlein, *ibid.* **20**, 964 (1968); W. E. Ellis *et al.*, *ibid.* **21**, 697 (1968); R. A. Jespersen *et al.*, *ibid.* **21**, 1368 (1968).

<sup>3</sup>L. David Roper, *Phys. Rev. Letters* **12**, 340 (1964).

<sup>4</sup>See, for example, T. C. Bacon *et al.*, *Phys. Rev.* **162**, 1320 (1967), for discussion and further reference.

<sup>5</sup>Philip M. Ogden *et al.*, *Phys. Rev.* **137**, B1115 (1965); Jerome A. Helland *et al.*, *ibid.* **134**, B1062 (1964); Gunnar Källén, *Elementary Particle Physics* (Addison Wesley Publishing Company, Inc., Reading, Mass., 1964), p. 72.

<sup>6</sup>J. D. Jackson, private communication.